Bulg. J. Phys. **42** (2015) 328–336

Description of Shape Transitions in Superheavy Nuclei within Covariant Density Functional Theory

G.A. Lalazissis[1], **V. Prassa**[2], **T. Nikšić**[2], **D. Vretenar**[2]

[1]Department of Theoretical Physics, Aristotle University of Thessaloniki, Thessaloniki Gr-54124, Greece

[2]Physics Department, Faculty of science, University of Zagreb, 10000 Zagreb, Croatia

Received *7 October 2015*

Abstract. A covariant energy density functional, adjusted to nuclear matter equation of state and empirical masses of deformed nuclei, is applied to study shapes of superheavy nuclei. Self-consistent mean field calculations predict a variety of spherical, axial and triaxial shapes of long lived superheavy nuclei. Alpha decay energies and half lives are compared with available experimental information. A microscopic quadrupole collective hamiltonian, based on the relativistic energy density functional, is used to study the effect of explicit treatment of collective correlations in the calculations of Q_α values and half lives.

PACS codes: 21.60.Jz, 21.10.Dr, 21.10.Re, 24.75.+i, 27.90.+b

1 Introduction

During the past few decades, important experimental progress on the mass limit of the nuclear chart has been made using compound nucleus reactions between the ^{48}Ca beam and actinide targets. A number of isotopes of new elements with the atomic number $Z = 113 - 118$ have been discovered, and new isotopes of $Z = 110$ and 112 have been identified, [1–11]. The decay energies and the resulting half-lives provide evidence of a significant increase of stability with increasing neutron number in this region of SHN. Theoretical studies predict that elements in this region should display rapid shape transitions, from prolate, through spherical, to oblate-deformed ground states [12–17]. These calculations of the structure of superheavy nuclei (SHN) can be divided into two categories: the traditional macroscopic-microscopic approach [12, 18–21], and the framework of self-consistent mean-field models (SCMF), based on realistic effective inter-nucleon interactions or energy density functionals, [12–16, 22–35]. The self-consistent mean-field (SCMF) models include an intuitive interpretation of

 1310–0157 © 2015 Heron Press Ltd.

results in terms of single-particle states and intrinsic shapes and offer a global description of nuclear properties across the nuclear landscape.The latter characteristic is important for extrapolations to regions of exotic short-lived nuclei far from stability for which few, if any, data are available. In addition, the SCMF approach can be extended beyond the static mean-field level to explicitly include collective correlations and, thus, perform detailed calculations of excitation spectra and transition rates.

In this study the framework of relativistic energy density functionals (REDF) is applied to an illustrative study of shape transitions and shape coexistence in superheavy nuclei (SHN) with $Z = 110 - 120$. The most important feature of functionals with manifest covariance is the natural inclusion of the nucleon spin degree of freedom, and the resulting nuclear spin-orbit potential which emerges automatically with the empirical strength. The model is first tested in calculations of ground state energies, quadrupole deformations, fission barriers, fission isomers, and α-decay energies of even-even actinide nuclei. We then apply the RHB framework based on the functional DD-PC1 [36] and a separable pairing interaction in a description of triaxially deformed shapes and shape transitions of even-even heavy and superheavy nuclei. The microscopic, REDF-based, quadrupole collective Hamiltonian model is used to study observables related to the effect of explicit treatment of collective correlations in the Q_α-energies in superheavy nuclei.

2 Fission Barriers of Actinides

The “double-humped" fission barriers of actinide nuclei provide an important test for nuclear energy density functionals. To illustrate the accuracy of the DD-PC1 functional in the calculation of ground-state properties of heavy nuclei, in Figure 1, we plot the potential energy curves of ^{236,238}U, ^{240}Pu, and ^{242}Cm, as functions of the axial quadrupole deformation parameter β_{20}. The deformation parameters are related to the multipole moments by the relation

$$\beta_{\lambda\mu} = \frac{4\pi}{3AR^\lambda}\langle Q_{\lambda\mu}\rangle \, .$$

To be able to analyze the outer barrier heights considering also reflection-asymmetric (octupole) shapes, the results displayed in this figure have been obtained in a self-consistent RMF plus BCS calculation that includes either triaxial shapes, or axially symmetric but reflection-asymmetric shapes. The interaction in the particle-hole channel is determined by the relativistic functional DD-PC1, and a density-independent δ-force is the the effective interaction in the particle-particle channel. The solid (black) curves correspond to binding energies calculated with the constraint on the axial quadrupole moment, assuming axial and reflection symmetry. The dot-dashed (blue) curves denote paths of minimal energy in calculations that break axial symmetry with constraints on quadrupole axial

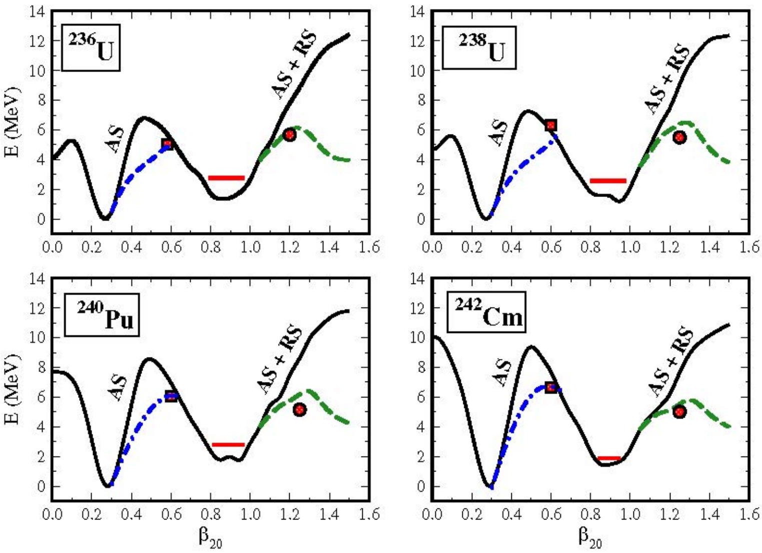

Figure 1. (Color online) Constrained energy curves of ^{236,238}U, ^{240}Pu, and ^{242}Cm, as functions of the axial quadrupole deformation parameter. Results of self-consistent axially and reflection-symmetric, triaxial, and axially reflection-asymmetric RMF+BCS calculations are denoted by solid (black), dot-dashed (blue), and dashed (green) curves, respectively. The red squares, lines, and circles denote the experimental values for the inner barrier height, the excitation energy of the fission isomer, and the height of the outer barrier, respectively. The data are from Ref. [38].

Q_{20} and triaxial Q_{22} moments. Finally, the dashed (green) curves are paths of minimal energy obtained in axially symmetric calculations that break reflection symmetry (constraints on the quadrupole moment Q_{20} and the octupole moment Q_{30}). The red squares, lines, and circles denote the experimental values for the inner barrier height, the excitation energy of the fission isomer, and the height of the outer barrier, respectively. The data are from Ref. [38].

The excitation energies of fission isomers are fairly well reproduced by the axially symmetric and reflection symmetric calculation, but the paths constrained by these symmetries overestimate the height of the inner and outer barriers. The inclusion of triaxial shapes lowers the inner barrier by ≈ 2 MeV, that is, the axially symmetric barriers in the region $\beta_{20} \approx 0.5$ are bypassed through the triaxial region, bringing the height of the barriers much closer to the empirical values. As shown in the figure, the inclusion of octupole shapes (axial, reflection-asymmetric calculations) is essential to reproduce the height of the outer barrier in actinide nuclei. A very good agreement with data is obtained by following paths through shapes with non-vanishing octupole moments.

3 Shape Transitions in Superheavy Nuclei

The variation of ground-state shapes is governed by the evolution of the shell structure of single-nucleon orbitals. In very heavy deformed nuclei the density of single-nucleon states close to the Fermi level is rather large, and even small variations in the shell structure predicted by different effective interactions can lead to markedly distinct equilibrium deformations.

To illustrate the rapid change of equilibrium shapes for the heaviest nuclear systems, Figure 2, displays the results of self-consistent triaxial RHB calculations of the energy surfaces in the $\beta - \gamma$ plane ($0 < \gamma < 60^0$) for isotopes in the α-decay chain of $^{300}120$ [37]. The heaviest systems display soft oblate axial

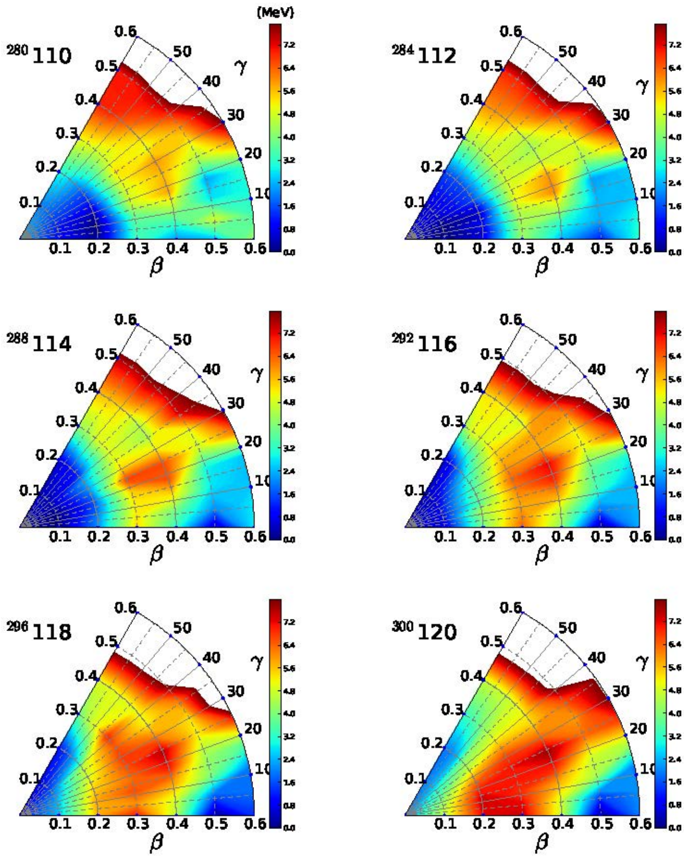

Figure 2. (Color online) Self-consistent RHB triaxial energy maps of the even-even isotopes in the α-decay chain of $^{300}120$ in the $\beta - \gamma$ plane ($0 \leq \gamma \leq 60°$). Energies are normalized with respect to the binding energy of the absolute minimum.

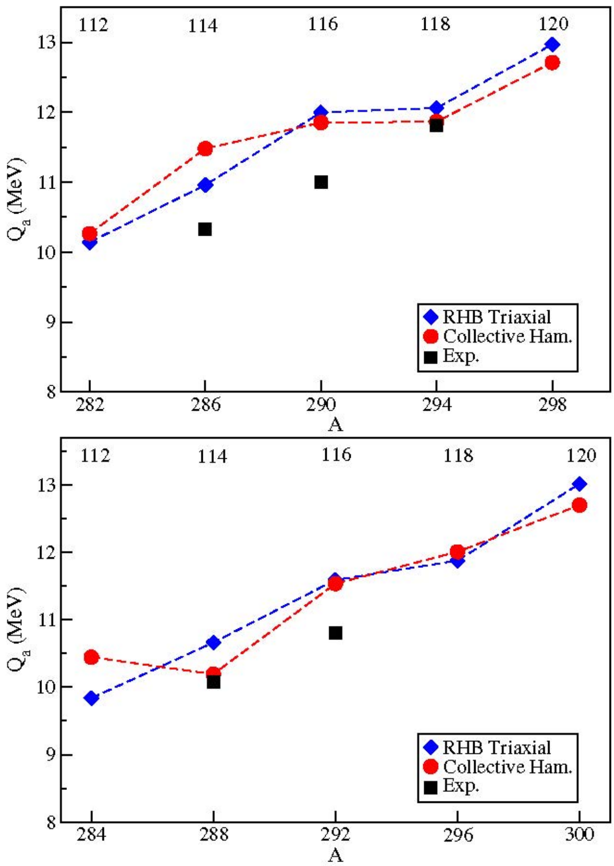

Figure 3. (Color online) Q_α values for the α-decay chains of $^{298}120$ (top) and $^{300}120$ (bottom). The theoretical values are calculated as the difference between the mean-field minima of the parent and daughter nuclei (blue diamonds), and as the difference between the energies of the 0^+ ground states of the quadrupole collective Hamiltonian (red circles). The data (squares) are from Ref. [4].

shapes with minima that extend from the spherical configuration to $\beta_{20} \approx 0.4$ ($Z = 120$) and $\beta_{20} \approx 0.3$ ($Z = 118$). We do not consider the deep prolate minima at $\beta_{20} > 0.5$ because the inclusion of reflection asymmetric shape degrees of freedom (octupole deformation) drastically reduces or removes completely the outer barrier. A low outer barrier implies a high probability for spontaneous fission, such that the prolate superdeformed states are not stable against fission. In contrast to the actinides shown in Figure 1, superheavy nuclei are actually characterized by a “single-humped" fission barrier. In the present implementation of the model triaxial and octupole deformations cannot be taken into account

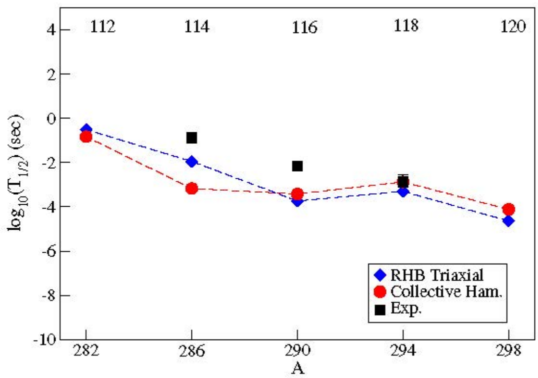

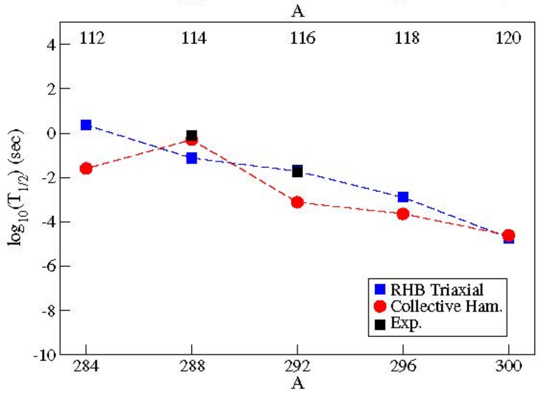

Figure 4. (Color online) Half-lives for the α-decay chains of $^{298}120$ (top) and $^{300}120$ (bottom). The theoretical values are calculated from a phenomenological Viola-Seaborg-type formula [12, 40], using the Q_α values from Figure 3. Diamonds correspond to values of Q_α calculated from mean-field RHB solutions, whereas circles denote half-lives computed using Q_α values determined by the 0^+ ground states of the quadrupole collective Hamiltonian. The data (squares) are from Ref. [4].

simultaneously. Reflection asymmetric shape degrees of freedom, however, play no role at small and moderate deformations that characterize ground-state configurations of the superheavy systems considered here. The intermediate nuclei with $Z = 116$ are essentially spherical but soft both in β and γ, whereas prolate deformed mean-field minima develop in the lighter systems with $Z = 114$, $Z = 112$ and $Z = 110$. The predicted evolution of shapes is consistent with results obtained using the self-consistent Hartree-Fock-Bogoliubov framework based on Skyrme functionals [13–15].

The two main decay modes in this region are α-emission and spontaneous fission. The theoretical values denoted by (blue) diamonds in Figure 3 correspond to transitions between the self-consistent mean-field minima on the triaxial RHB energy surfaces. Such a calculation does not explicitly take into account collective correlations related to symmetry restoration and to fluctuations in the collective coordinates β and γ. Physical transitions occur, of course, not between mean-field minima but between states with definite angular momentum. For this reason we have also used a recent implementation of the collective Hamiltonian based on relativistic energy density functionals [39], to calculate α-transition energies between ground states of even-even nuclei ($0^+ \rightarrow 0^+$ transitions). The (red) circles in Figure 3 denote the Q_α values, computed for transitions $0^+_{\rm g.s.} \rightarrow 0^+_{\rm g.s.}$ between eigenstates of the collective Hamiltonian. The differences with respect to mean-field values are not large, especially for the heaviest, weakly oblate deformed or spherical systems. For the lighter prolate and more deformed nuclei, the differences can be as large as the deviations from experimental values. The trend of the data is obviously reproduced by the calculations, and the largest difference between theoretical and experimental values is less than 1 MeV.

Alpha-decay half-lives are calculated using a simple five-parameter phenomenological Viola-Seaborg-type formula [12, 40]. The parameters of this formula were adjusted to experimental half-lives and Q_α values of more than 200 nuclei with $Z = 84 - 111$ and $N = 128 - 161$ [40]. Using the theoretical Q_α values plotted in Figure 3 as input, the resulting half-lives are compared to available data [4] in Figure 4. A rather good agreement with experiment is obtained for both decay chains.

4 Conclusions

In this work, the relativistic nuclear energy density functionals (EDFs) framework has been applied to a study of deformation effects and shapes of superheavy nuclei. The microscopic self-consistent calculation is based on the EDF DD-PC1 [36], and a separable pairing interaction, used in the relativistic Hartree-Bogoliubov (RHB) model.

This analysis demonstrates the potential of the semi-empirical REDFs for studies of shape coexistence and triaxiality in the heaviest nuclear system, including the explicit treatment of collective correlations using a microscopic collective Hamiltonian. This opens the possibility for a more detailed analysis of this region of SHN, including all presently known nuclides with $Z = 110 - 118$, as well as spectroscopic studies of nuclei with $Z > 100$.

Acknowledgments

Support by the Bulgarian National Science Fund (BNSF) under Contract No. DFNI-E02/6 is gratefully acknowledged.

References

[1] Yu.Ts. Oganessian and V.K. Utyonkov (2015) *Rep. Prog. Phys*. **78** 036301.
[2] V.K. Utyonkov *et al.* (2015) *Phys. Rev. C* **92** 034609.
[3] J. Khuyagbaatar *et al.* (2014) *Phys. Rev. Lett*. **112** 172501.
[4] Yu.Ts. Oganessian (2007) *J. Phys. G: Nucl. Part. Phys*. **34** R165.
[5] S. Hofmann *et al.* (2007) *Eur. Phys. J. A* **32** 251.
[6] Yu.Ts. Oganessian *et al.* (2010) *Phys. Rev. Lett*. **104** 142502.
[7] Yu.Ts. Oganessian *et al.* (2011) *Phys. Rev. C* **83** 054315.
[8] Yu.Ts. Oganessian *et al.* (2012) *Phys. Rev. Lett*. **108** 022502.
[9] L. Stavsetra *et al.* (2009) *Phys. Rev. Lett*. **103** 132502.
[10] Ch.E. Düllmann *et al.* (2010) *Phys. Rev. Lett*. **104** 252701.
[11] P.A. Ellison, *et al.* (2010) *Phys. Rev. Lett*. **105** 182701.
[12] A. Sobiczewski and K. Pomorski (2007) *Prog. Part. Nucl. Phys*. **58** 292.
[13] S. Čwiok, J. Dobaczewski, P.-H. Heenen, P. Magierski, W. Nazarewicz (1996) *Nucl. Phys. A* **611** 211.
[14] S. Čwiok, P.-H. Heenen, W. Nazarewicz, Nature 433, 705 (2005).
[15] S. Čwiok, W. Nazarewicz, and P.-H. Heenen (1999) *Phys. Rev. Lett*. **83** 1108.
[16] P.-H. Heenen and W. Nazarewicz (2002) *Europhys. News* **33** 1.
[17] P. Jachimowicz, M. Kowal, and J. Skalski (2011) *Phys. Rev. C* **83** 054302.
[18] M. Brack, J. Damgaard, A.S. Jensen, H.C. Pauli, V.M. Strutinski, C.Y. Wong (1972) *Rev. Mod. Phys*. **44** 320.
[19] P. Möller and J.R. Nix (1994) *J. Phys. G: Nucl. Part. Phys*. **20** 1681.
[20] P. Möller, J.R. Nix, W.D. Myers, and W.J. Swiatecki (1995) *At. Data Nucl. Data Tables* **59** 185.
[21] A. Sobiczewski (1994) *Phys. Part. Nucl*. **25** 119.
[22] G.A. Lalazissis, M.M. Sharma, P. Ring, and Y.K. Gambhir (1996) *Nucl. Phys. A* **608** 202.
[23] M. Bender, K. Rutz, P.-G. Reinhard, J.A. Maruhn, and W. Greiner (1998) *Phys. Rev. C* **58** 2126.
[24] M. Bender, K. Rutz, P.-G. Reinhard, J.A. Maruhn, and W. Greiner (1999) *Phys. Rev. C* **60** 034304.
[25] J.-F. Berger, L. Bitaud, J. Dechargé, M. Girod, and K. Dietrich (2001) *Nucl. Phys. A* **685** 1.
[26] M. Warda, J.L. Egido, L.M. Robledo, and K. Pomorski (2002) *Phys. Rev. C* **66** 014310.
[27] S. Goriely, M. Samyn, P.-H. Heenen, J.M. Pearson, and F. Tondeur (2002) *Phys. Rev. C* **66** 024326.
[28] M. Bender, P.-H. Heenen, and P.-G. Reinhard (2003) *Rev. Mod. Phys*. **75** 121.
[29] T. Bürvenich, M. Bender, J.A. Maruhn, and P.-G. Reinhard (2004) *Phys. Rev. C* **69** 014307.
[30] J.-P. Delaroche, M. Girod, H. Goutte, J. Libert (2006) *Nucl. Phys. A* **771** 103.
[31] J.A. Sheikh, W. Nazarewicz, and J.C. Pei (2009) *Phys. Rev. C* **80** 011302.
[32] J. Erler, P. Klüpfel, and P.-G. Reinhard (2010) *Phys. Rev. C* **82** 044307.

[33] E.V. Litvinova and A.V. Afanasjev (2011) *Phys. Rev. C* **84** 014305.

[34] E.V. Litvinova (2012) *Phys. Rev. C* **85** 021303.

[35] H. Abusara, A.V. Afanasjev, and P. Ring (2012) *Phys. Rev. C* **85** 024314.

[36] T. Nikšić, D. Vretenar, and P. Ring (2008) *Phys. Rev. C* **78** 034318.

[37] V. Prassa, T. Nikšić, G.A. Lalazissis, D. Vretenar (2012) *Phys. Rev. C* **86** 024317.

[38] R. Capote, M. Herman, P. Obložinský, P.G. Young, S. Goriely, T. Belgya, A.V. Ignatyuk, A.J. Koning, S. Hilaire, V.A. Plujko, M. Avrigeanu, O. Bersillon, M.B. Chadwick, T. Fukahori, Zhigang Ge, Yinlu Han, S. Kailas, J. Kopecky, V.M. Maslov, G. Reffo, M. Sin, E.Sh. Soukhovitskii, and P. Talou (2009) *Nucl. Data Sheets* **110** 3107; Reference Input Parameter Library (RIPL-3) [http://www-nds.iaea.org/RIPL-3/].

[39] T. Nikšić, Z.P. Li, D. Vretenar, L. Próchniak, J. Meng, and P. Ring (2009) *Phys. Rev. C* **79** 034303.

[40] A. Parkhomenko and A. Sobiczewski (2005) *Acta Phys. Pol. B* **36** 3095.